Biol. Cybernetics 28, 1–14 (1977)

Biological Cybernetics

Afferent Geometry in the Primate Visual Cortex and the Generation of Neuronal Trigger Features*

E. L. Schwartz

Brain Research Laboratories of Psychiatry, New York University Medical School, New York, USA

Abstract. In previous work, it was suggested that the sequence regularity property of cortical neurons could be accounted for if the local geometric structure of the cortex were a recapituation of the global complex logarithmic structure of the retinotopic mapping. This model is developed in detail: the excitatory and inhibitory structure of cortical receptive fields may be approximated by a complex logarithmic local geometry, coupled with an intra-cortical lateral inhibition operator which may flow unidirectionally yet still create "rotating" receptive field structure. The direction of intra-cortical lateral inhibition follows the borders of cortical ocular dominance columns, which are the approximate images under the global complex logarithmic mapping, of exponentially spaced, horizontal straight lines in the visual field. Two different topological structures are discussed for the local cortical manifold. The binocular trigger features of cortical neurons follow from the same geometric model, and the ratio of binocular to monocular cortical cells is related to the size and shape of cortical dendritic tree's by an application of integral geometry. Recent results in optical pattern recognition are cited to suggest that the rotation and size invariant properties of the cortical map are essential to any cross-correlational basis for stereopsis. Finally, a meromorphic function is presented which is both locally and globally complex logarithmic in its structure, and therefore represents the model presented in this and previous papers in a concise mathematical form. This function is closely related to the description of a Karman vortex pattern, in fluid mechanics, and leads to the suggestion that the boundary conditions of layer IV of the cortex (i.e. periodic ocular dominance columns) are causally related to the existence of sequence regularity in the cortex. The developmental implications of this statement are that the specification of neural connections in the cortex may follow directly, both locally and globally, from the detailed nature of the cortical boundary conditions (i.e. anatomy), coupled with general physico-mathematical considerations of continuity and differentiability in the neural fiber flow.

* This work was supported by Grants 1-F32MH0536701 from A.D.A.M.H.A. and BMST5-02819 from N.S.F.

Introduction

The global analytic structure of the retinotopic mapping of the primate cortex has been characterized by a complex logarithmic mapping of the retinal surface to the cortical surface; the receptotopic structure of the secondary and medial visual cortex, the inferior pulvinar nucleus, and the somatotopic mapping (cortical area $S-1$) have a similar analytic structure (Schwartz, 1976, 1977a). In this work, it was pointed out that the description of neuronal mappings via analytic functions (conformal mappings) has a simple developmental interpretation: analytic functions, such as the complex logarithm, represent "potential flow" on surfaces, subject to boundary conditions imposed by the "shape" of the surface. Thus, the development of specific neuronal mappings may be "encoded" by minimal rules such as those describing the flow of fluids, the diffusion of chemical substances, etc. This idea was developed in detail in subsequent work (Schwartz, 1977b) where Dirichlet's Principle was used to demonstrate that the minimization of the average magnitude of the anatomical magnification factor (per unit area) is sufficient to encode the structure of a detailed receptotopic mapping, based on the shape or boundary conditions of the available tissue surfaces. In the monkey, this follows from the demonstration that the density of retinal ganglion cells implies an annular domain which is logarithmically structured, as originally suggested (in the cat) by Fischer (1973). The cortical domain is characterized as a rectilinear strip, and the retinal annulus is conformally equivalent to the cortical strip,

under the complex logarithmic mapping. In the goldfish, the retina may be characterized as a disk (constant cell density) and the optic tectum as an ellipse. The unit disk is mapped to an ellipse by a certain Jacobian elliptic conformal mapping, and the level lines of this function are in agreement with the experimentally determined retino-tectal mappings of the goldfish. Specific experimental tests of this theory are outlined in the same paper. The present paper is a detailed development of a second suggestion presented in Schwartz (1976, 1977a). The sequence regularity property of the visual cortex of the primate (and the cat) suggests that the local structure of the cortical map is also described by the complex logarithm function: the cortex is a concatenated logarithmic map. This follows because the angle of orientation tuning of cortical cells rotates through equal angular increments as an electrode traverses equal linear steps across the surface of the cortex. Since the complex logarithm function assigns a polar angle in the visual field to a linear coordinate in the cortex, it is intuitively evident that dendritic summation of an afferent input to the cortex that is locally logarithmic in its structure would provide this sequence regularity property. The detailed presentation of this statement requires a discussion of intra-cortical inhibition, the nature of the images of the dendritic tree's of cortical cells, the topological structure of the local cortical mapping, and a model for the "packing" of adjascent hypercolumn mappings in the cortex.

In the present paper, a geometric model for the local structure of the afferent input to the visual cortex is presented; this model accounts in a logically consistent way for a variety of anatomical and physiological features of the visual cortex, and leads to the following statements: 1) The borders of the ocular dominance columns in the primate are the approximate mapping under the complex logarithm of horizontal, exponentially spaced lines in the visual field; 2) The images of the dendritic tree's of cortical cells, under the local logarithmic mapping, are not particularly elongated, in agreement with experimental data from the cat and the primate, which implies: 3) Intra-cortical inhibition must be responsible for the existence of "line tuning" and inhibitory sidebands, as suggested by Creutzfeld et al. (1974), and Schiller et al. (1976b). However, since the angle of both the excitatory center and the inhibitory surround rotates (sequence regularity), the intra-cortical connections responsible for this lateral inhibition must be highly "tangled", unless; 4) The local structure of the cortical mapping is a recapitulation of the global logarithmic structure, which causes the afferent input to effectively "rotate", allowing intra-cortical inhibitory connections to lie parallel to one another. This directional intra-cortical inhibition is mathematically modeled by a modification of the Laplacian operator (which becomes a "directional derivative"), and the direction of this inhibition is suggested to lie parallel to the ocular dominance column boundaries; 5) Orientation columns are therefore a joint product of directional lateral inhibition, and the locally logarithmic structure of the cortex: they need not have an observable anatomical substrate as "columns". 6) A simple application of integral geometry ("Bufon's Needle") allows a calculation of the ratio of binocular to monocular cortical cells, which is in good agreement with experiment, and which makes definite predictions for the perimeter of the dendritic tree's of cortical "S" and "CX" type cells. 7) The topological structure of a cortical hypercolumn is discussed, and the possibility is raised that the standard cylindrical Riemann surface of the logarithm function may have to be modified to a nonoriented cylindrical surface for the local cortical map, in order to achieve a symmetric hypercolumn structure. This gives some insight into Werner's (1970) demonstration of the non-oriented topological structure of the somatosensory cortex: higher topological structure, in a biological context, may arise from the need to satisfy simple boundary conditions and symmetry requirements. 8) The binocular trigger features of the primate cortex, as measured by Hubel and Wiesel (1970), follow from the model of cortical geometry. A formula is derived relating binocular disparity to the cortical magnification factor, the amount of shift of neighboring receptive fields, and the size of a "hypercolumn". The large magnification factor for the parafoveal striate cortex predicts values of binocular disparity tuning that are extremely small, possibly explaining the lack of observed disparity tuning in the primate striate cortex. 9) Since the monocular and binocular trigger features of the visual cortex may be accounted for by a simple geometric structuring of the afferent input, then the identification of the psychological process of "feature extraction" with the neuronal trigger features is called into question. The relationship between structure and function in the cortex might be more aptly described in terms of "computational geometry" rather than "neuronal feature extraction". This (Gestalt) approach to the psychology of the visual cortex is supported by 10) Recent results in optical pattern recognition which indicate that if stereopsis is to depend on cross-correlation between the left and right eye input, then the size and rotation invariant properties of the complex logarithmic retinotopic mapping (Chaikin and Weiman, 1977; Casasent and Psaltis, 1977; Schwartz, 1977a) are critical to maintaining a reasonable signal to noise ratio. 11) A mermomorphic function is presented which represents a concatenated complex logarithmic map, i.e. it is locally and globally logarithmic. This map concisely summarizes the geometric model presented in this paper, and represents a convenient mathematical

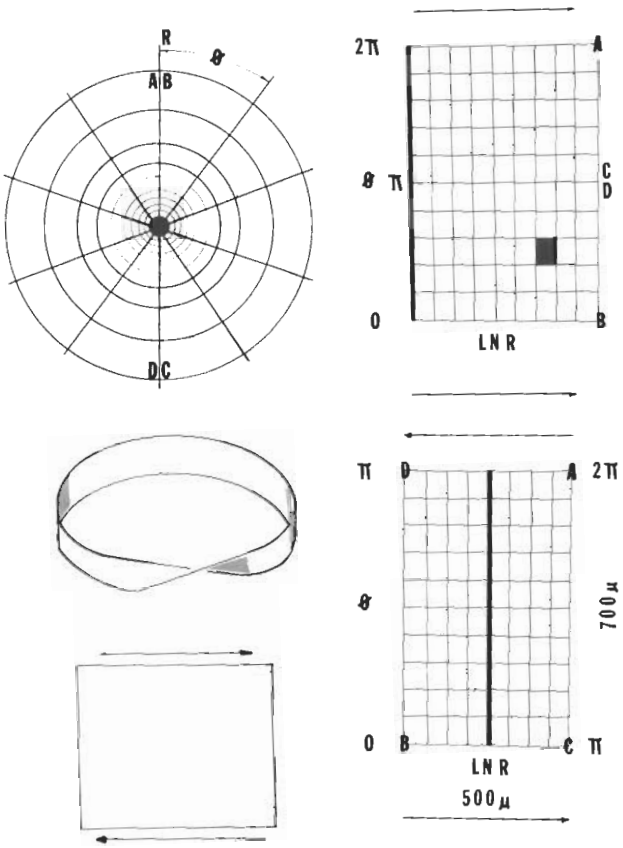

Fig. 2. On the top left is shown the iso-density lines ot the complex logarithmic retinal cell density. The polar coordinates r and $\emptyset$ are shown, and the black area at the center corresponds to the region where retinal ganglion cell density (X type ganglion cells) falls rapidly in both the cat and the monkey: this is the singularity of the logarithm function. On the right is the mapping of the retina, under the complex logarithm function. The small shaded area is meant to represent a "hypercolumn", which is the basic unit of the cortical mosaic. This mapping represents a logarithmic potential on a surface of cylindrical topology (the Points A, and B are the same point). On the bottom is shown an alternate topology: this figure represents a logarithmic mapping on a nonorientable cylinder, i.e. a Moebius strip, which is shown at the bottom left, (compare Points A–D in the retina, and on the two logarithmic mappings). The dimensions of 500 μ by 700 μ are estimates of the size of one half of a hypercolumn from the data of Hubel and Wiesel (1974)

The vertical meridian (V), the horizontal meridian (H) and the approximate foveal representation (F) are shown in the figure. Levay et al. remark that the representation of the ocular dominance columns tend to run along lines that are parallel to the horizontal meridian for the central 10° of the field. In Figure 1 is shown the mapping, under the complex logarithm function, of exponentially spaced, horizontal lines. There is suggestive agreement between these figures.

The mapping function of Figure 1 is $\ln(z+1)$, which is regular at the origin ($z=0$), which is essentially identical to $\ln(z)$ beyond the central 1–2° of visual field, which provides an analytic representation for the (unmapped) central 1° of field, and which duplicates the "C" shaped boundary of the cortex, along the lunate sulcus (the representation of the vertical meridian in the primate).

Levay et al. (1975) have suggested that the equal width of the ocular dominance strips is due to a competition for space between the left and right eye maps which tends to equalize the area of the two representations, causing a random consolidation of neighboring columns, with the consequent production of "blind endings", as in Figure 1. Nevertheless, the fact that the ocular dominance columns run along trajectories which are approximately predictable, based on the complex logarithm function, is fundamental. It will become clear that the borders of the ocular dominance columns play a basic role in "organizing" the local logarithmic structure of the cortex in the present model: intra-cortical lateral inhibition and sequence regularity run parallel to these borders, while binocular summation runs perpendicular to them. The ocular dominance columns provide the link between the axes of the global and the local mappings of the cortex.

The Global and Local Cortical Mappings: Analytic and Topological Structure

Figure 2 illustrates the analytic and topological structure of the global logarithmic mapping.

The circular pattern on the left is identified with the retina (visual field). The cell density of X type ganglion cells in the cat (Fischer, 1973; McIlwain, 1976) and the monkey retina (Rolls and Cowey, 1970) is described by an inverse square law. Ganglian cell density is inversely proportional to the square of the eccentricity. The inverse square law is the same as that which describes the fields of classical potential theory (electrostatic, gravitational, etc.). A planar problem in electrostatics (the potential around a line charge) is described by a complex logarithmic potential function because of the inverse square dependence of the field (Panafsky and Phillips, 1962). In an exactly analgous manner, a complex logarithmic density potential can be introduced for the retina (Schwartz, 1977b). The rectangular strip on the right of Figure 2 shows the mapping of the retina to the cortex, under the complex logarithm function. A rectangular strip is conformally equivalent (Ahlfors, 1966) to the retinal annulus. This mapping provides a system which is isotropic in retinal cell density (Fischer, 1973) and provides an approximate description of the actual retinotopic mapping of the primate cortex (Schwartz, 1976, 1977a).

The topological structure of the complex logarithmic mapping is that of a cylinder. In Figure 2 (right), the rays $\emptyset=0$ and $\emptyset=2\pi$ are located at opposite ends of the

summary of the anatomical and physiological features of striate cortex in the primate. 12) It is pointed out that the previously mentioned function is closely related to the mathematical description of a Karman vortex street pattern in two dimensional fluid mechanics. This provides possible insight into the nature of cortical development, since it extends a previously developed model of neural development, based on irrotational fluid flow (via the Laplace equation), to the much more sophisticated, rotational flow represented by the Navier-Stokes equation. Based on this observation, it is argued that the encoding of sequence regularity in the cortex may follow directly from the boundary conditions of the local cortical anatomy (i.e. the existence of ocular dominance columns), just as the global retinotopic map has been suggested to follow from the global retinal and cortical "shape" (Schwartz, 1977b). Thus, a single unified mathematical approach may be capable of summarizing a wide range of disparate aspects of striate cortex phenomenology.

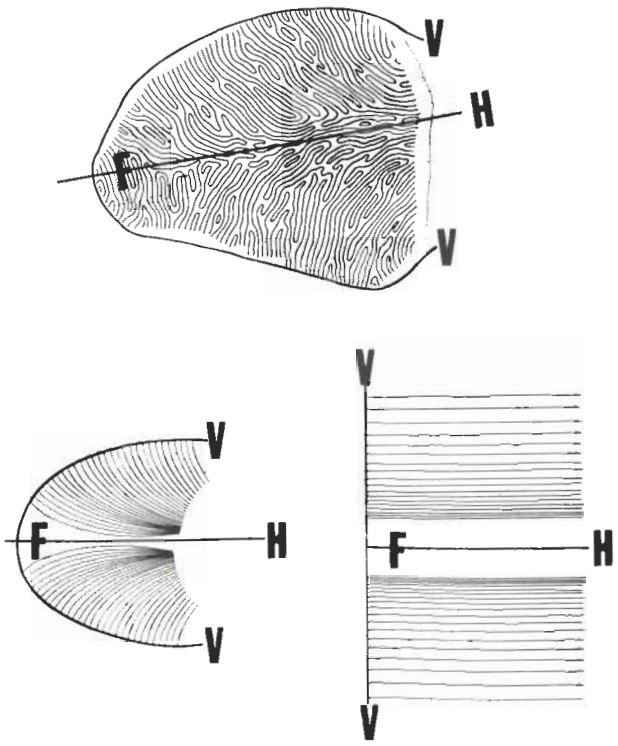

Fig. 1. On top is shown the reconstruction of tangential sections of the striate cortex (silver stain) of Levay et al. (1975). Alternate bands represent left eye and right eye input. The approximate representations of the vertical meridian (V), the horizontal meridian (H) and the foveal representation (F) have been added to the original in order to facilitate comparison with the theoretical version shown below. This is the mapping, under the function $\ln(z+1)$ of a series of parallel exponentially spaced horizontal straight lines in the visual field. The exponential spacing was chosen in order to provide equal width of the "ocular dominance columns" at their intersection with the representation of the vertical meridian ("V" in the figure)

Dendritic Summation in the Visual Cortex

Colonnier (1964) studied tangential sections of Golgi stained rat, cat and monkey visual cortex. He found that the shape of the dendritic trees of the cortical cells was elongated, with a typical ratio of 1.5:1. The long axis was predominantly parallel to the representation of the vertical meridian (i.e. the lunate sulcus in the primate). Since Levay et al. (1975) remark that the ocular dominance column boundaries run primarily in a direction parallel to the horizontal meridian, for the central 10° of field, the orientation of the cortical dendritic trees is primarily perpendicular to the ocular dominance column boundaries. Based on the observed dendritic asymmetry, Colonnier suggested that dendritic summation of cortical afferents could explain the fact that cortical cells respond to elongated stimuli in the visual field (i.e. edges, or lines). Hubel and Wiesel (1962) have suggested that convergence of a line of geniculate cells onto a single cortical cell could explain this line tuning property of cortical cells. In later work, McIlwain (1976) pointed out that dendritic summation of an anisotropic distribution of cortical (or tectal) afferents could yield images of dendritic tree's that were elongated.

However, Creutzfeld et al. (1974) have found that the distribution of EPSP's arriving at a single cortical cell (in the cat) suggests a circularly symmetric excitatory field, and concluded that the highly elongated nature of many cortical receptive fields, as well as the presence of inhibitory sidebands and directional selectivity, must depend on intra-cortical lateral inhibition. Since the angle of orientation of the cortical receptive fields rotates as one traverses the cortex the intracortical connections responsible for orientation tuning must "rotate" also. An alternative possibility is that the direction of intra-cortical lateral inhibition is constant, but that the underlying mapping of cortical afferents effectively "rotates". This suggestion, implicit in the proposed logarithmic structure of the cortex, will now be developed in detail.

Ocular Dominance Column Trajectories

The characterization of the global retinotopic mapping of the cortex by the complex logarithm function was based on physiological measurements (magnification factor and the mapping of global landmarks). Further support for this characterization comes from the histological reconstruction of cortical ocular dominance column trajectories of Levay et al. (1975). Ocular dominance columns are strips of cortex, approximately 500 μ wide, which alternately represent left eye and right eye input to the cortex. Levay et al. (1975) have reconstructed the ocular dominance column pattern of the cortex, and the results of this are shown in Figure 1.

cortical strip, but are actually idential points in the retina (or visual field). The cylinder forms a standard Riemann surface for the logarithm function (Springer, 1953). Anatomically, the two hemispheric representations of the cortex are joined by the corpus callosum about the representation of the vertical meridian (Hubel and Wiesel, 1967), and this supports the interpretation of the cortical topology as that of a cylinder.

In Figure 2, a small patch of the global cortical map is shaded, and this is meant to suggest the basic hypercolumn unit of cortical structure. A complete range of angular orientations is represented by a hypercolumn, as well as both left and right eye input (Hubel and Wiesel, 1974). For the moment, the analytic structure of half of a hypercolumn is addressed (i.e. the geometric structure of a single ocular dominance column); the packing of adjacent ocular dominance columns will be discussed in relation to binocular trigger features. Sequence regularity implies that the analytic structure of the hypercolumn is described by the complex logarithm function (Schwartz, 1976, 1977a), and a possible description would be simply a reiteration of the global topology and geometry, as in the top of Figure 2. However, it may be observed that this figure is asymmetric: the foveal representation is located at the lateral edge of the cortex. A symmetric complex logarithmic mapping may be obtained by altering the local topological structure of the cortical surface, from an orientable cylinder to a non-orientable cylinder. This is achieved by "cutting" the mapping at the top of Figure 2, about the line $\emptyset = \pi$, and folding it over, back and up.

The result of this operation is shown at the bottom of Figure 2; the Points A–D, have been identified in both figures. The result of this procedure is that the center of the local receptive field is mapped to the center strip of the hypercolumn. The topological identification of the resulting (local) cortical manifold as a non-orientable cylinder is proven by identifying the points at the top and bottom of the map (bottom of Fig. 2). The opposite direction of these "identified" points is the standard topological description of a Moebius strip (Spivak, 1970), which is also shown in the figure, for reference.

The two mappings of Figure 2 differ only in the underlying topological structure of the manifolds in which they are embedded. The global logarithmic mapping is described by the cylindrical topology of the top of Figure 2. *Either of the two mappings of Figure 2 could supply a sequence regularity property, via dendritic summation.* However, the non-oriented version (Moebius strip) of the logarithmic mapping will be used in the following discussion, because it is symmetric about the local receptive field center.

The "cylindrical" topology of Figure 2 would lead to cortical receptive fields that were coincident with the *radii* of the circle centered about the local r.f. center; the "Moebius Cylinder" of Figure 2 would lead to receptive fields that were co-incident with the *diameters* of the same circle. Therefore, the detailed nature of sequence regularity (Hubel and Wiesel, 1974) would allow a choice between these possibilities. Also, the "Moebius" version of the logarithmic mapping should be understood as a "construction", as indicated in Figure 2, rather than a well defined mathematical mapping, thus allowing the evasion of the question of defining a Riemann surface on a non-orientable manifold [formally, Riemann surfaces must be orientable (Springer, 1953)].

The introduction of surfaces of higher topological structure in a biological context may seem exotic. However, there is a precedent for considering higher topological surfaces in the primate sensory system. Werner has demonstrated (1970) that the topological structure of the somatosensory cortex is that of a non-oriented torus, i.e. a Klein Bottle. Moreover, the analytic structure of this mapping is similar to that of the complex logarithm (Schwartz, 1977a). In this context, the proposed description of the local structure of the visual cortex is not so far-fetched; in fact, some insight may be shed on the problem of the topological constraints that are associated with receptotopic mappings. In order to satisfy boundary conditions (of symmetry, with neighboring tissue surfaces, etc.), higher order topological manifolds may be relevant to the description of neuronal mappings.

Figure 2 (bottom) shows the proposed geometric structure for a hypercolumn. A question naturally arises concerning the anatomical and physiological identification of this local mapping in the retinal (or lateral geniculate) plane. The basic columnar unit of the lateral geniculate is the direction column. The distribution of receptive field centers in a direction column is denser in the center, tapering off in a gradual (Gaussian) circularly symmetric distribution (Sanderson, 1971).

This argument suggests the following analogy: *retina:cortex: :direction column: hypercolumn.* Regardless of whether or not this analogy is valid, the local mapping of the cortical afferents, described by Figure 2, succeeds in providing a variety of neuronal trigger features of the cortex, as will now be formally demonstrated.

Dendritic Images under the Local Logarithmic Mapping

Colonnier (1964) measured the shapes and sizes of the dendritic tree's of cortical stellate and pyramidal cells in the rat, the cat, and the monkey. For cortical stellate

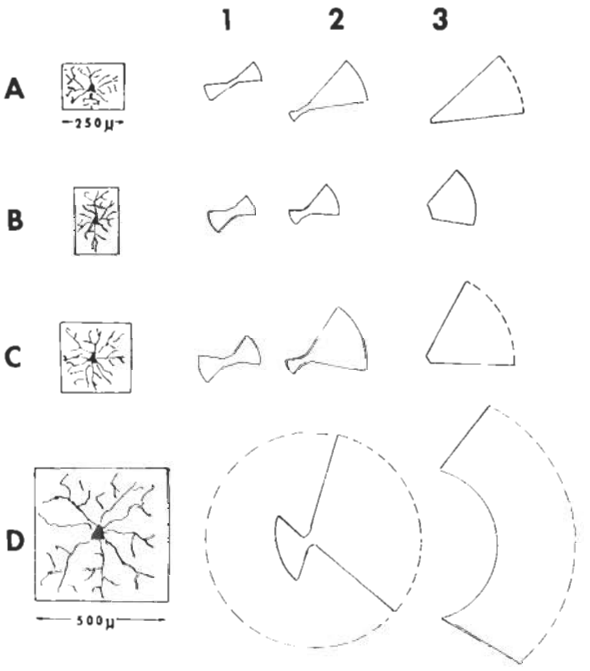

Fig. 3. The rectangles A–D, are idealizations of tangential sections of cortical stellate and pyramidal cells, after Colonier. "Cell" D is atypically large, and is included for that reason. The images of these "cells" under the logarithmic mapping of Figure 2 (bottom) are shown in Columns 1–3, which represent lateral distance from the center of the hypercolumn, in 75 μ steps. Movement in the vertical dimension causes identical images, with a rotation proportional to the vertical movement. The images (excitatory field centers) are not particularly sensitive to the size, shape or position of the "cell", except for the largest cell Type D

cells, he reported the typical shape to be "cruciform", with the long axis usually more than 1.5 times the length of the short axis. The average length of the long axis was 136.7 μ (standard deviation 43 μ) for uncut dendritic tree's; this criterion of "uncut" biases the sample towards smaller cells, and Colonnier reports a grand average of 266.4 μ (standard deviation 120.4 μ) for the size of the dendritic tree's of stellate cells. In the following discussion, a "typical" cortical dendritic tree will be characterized as a rectangle, with an aspect ratio of 1.5:1, and with the long side equal to 250 μ. Thus, the "typical" cells of Figure 3 are meant to conform roughly to Colonnier's data. Cells A and B represent an elongated dendritic tree of aspect ratio (1.5:1) whose long axis (250 μ) is oriented parallel to the horizontal meridian. Cell "C" is a symmetric cell of approximately the same size, and Cell "D" represents a dendritic tree that is larger than average (500 μ). The Nos. 1–3 refer to distance from the center of the hypercolumn. Cell 1 is located at the center of the hypercolumn (Fig. 1) and Cells 2 and 3 are 75 and 150 μ from the center respectively, measured along the horizontal coordinate of Figure 1 (bottom). The shapes of these "cells" are mapped in polar coordinate sectors by the logarithmic mapping, and shown in Figure 3. The general tendency of these dendritic tree images is to be of roughly the same degree of elongation as the cell shape itself. *The anisotropy of the mapping does not contribute greatly to any elongation of the dendritic tree images*, except for the largest cell, "D". In this case, the cell size is of the same order of magnitude as the size of the hypercolumn, and a dendritic tree image is formed with a marked elongation in the vertical direction. It is interesting to point out that this image resembles the shape of a hypercomplex receptive field (Hubel and Wiesel, 1962) i.e. it is large and has a distinct angular "kink" in it. The principle conclusion to make from Figure 3 is that, given the scale of a cortical hypercolumn based on the data of Hubel and Wiesel (1974), and the average cells sizes measured by Colonnier (1964) *the anisotropy of the local structure of the cortex is not sufficient, except for the larger cells that may be present, to provide a significant elongation of the receptive field shape.*

Intra-Cortical Lateral Inhibition

The dendritic images of Figure 3 are in agreement with the shape of the excitatory centers of cortical receptive fields. Creutzfeldt et al. (1974) found, in the cat, that the excitatory centers of cortical cells tended to be roughly circular to elliptical, with eccentricities in the range of 1–1.5. Schiller et al. (1976a) found, in the primate, that the excitatory centers of cortical receptive fields also were roughly circular to elliptical. The elongated nature of cortical receptive fields that is typically recorded with elongated stimuli is to some extent an artifact of the stimuli themselves, and must depend on the presence a of neural mechanism in addition to dendritic summation of excitatory input. Creutzfeldt et al. (1974) and Schiller et al. (1976b) have proposed intra-cortical inhibitory mechanisms to account for cortical line tuning. However, the nature of this intra-cortical inhibition, regardless of the details of its neural substrate, seems to be tightly constrained by the geometric fact of sequence regularity.

Lateral inhibition is often modeled mathematically by the "Laplacian", which is the simplest second order isotropic difference operator:

$$\nabla^2 = \frac{\partial^2}{\partial x^2} + \frac{\partial^2}{\partial y^2}. \tag{1}$$

However, the Laplacian represents isotropic lateral inhibition; in order to model directional lateral in-

hibition, a directional derivative operator may be defined as follows:

$$\nabla_\theta = \cos\theta \hat{i}\,\frac{\partial}{\partial x} + \sin\theta \hat{j}\,\frac{\partial}{\partial y}$$
$$\nabla_\theta^2 = \cos^2\theta\,\frac{\partial^2}{\partial x^2} + \sin^2\theta\,\frac{\partial^2}{\partial y^2}. \quad (2)$$

The angle θ determines the amount of anisotropy of the lateral inhibition. For $\theta = \pi/2$, the operator of (2) reduces to a simple differencing parallel to the y axis, which is identified as the local axis along which orientation tuning is changing. Hubel and Wiesel (1972) have suggested that this direction may lie parallel to the ocular dominance column-boundaries. Although this statement has not been experimentally verified, it is supported by the development of binocular trigger features that is presented later in this paper. Thus, the direction of intra-cortical inhibition, which is parallel to the direction of "sequence regularity", is assumed to lie parallel to the ocular dominance column boundaries.

A simple graphic simulation of intra-cortical inhibition under this assumption is shown in Figure 4. A narrow excitatory center, flanked by larger inhibitory bands is produced. As Creutzfeldt et al. (1974) have emphasized, intra-cortical lateral inhibition seems to be necessary to produce elongated receptive fields, inhibitory sidebands, and directional sensitivity. The principal contribution of the present work to this question is to provide a geometrical interpretation for this lateral inhibition operation, and in pointing out the potential relationships between the direction of intra-cortical inhibition, sequence regularity, and the ocular dominance column-boundaries.

Schiller et al. (1976b) have suggested three possible alternatives for the neuro-physiological basis of directional cortical inhibition: 1) dendritic summation along oriented dendritic trees; 2) anisotropic distribution of inhibitory synapses; and 3) anisotropic geometry of the axons of inhibitory interneurons. The first of these suggestions may be related to the cruciform shape of the dendritic trees of cortical neurons reported by Colonnier (1964). Since the long axes of the dendritic tree are oriented predominantly parallel to the representation of the vertical meridian (according to Colonnier) then these axes lie approximately perpendicular to the ocular dominance column-boundaries (Fig. 1). The remaining perpendicular segment of the dendritic tree then must lie predominantly parallel to the ocular dominance column-boundary, and would be a candidate for suggestion (1) above. In the motor cortex, the presumed interneurons are basket cells, and their axons follow long parallel trajectories (Marin-Padilla, 1970). Should a similar axon geometry be found in the visual cortex, it could provide a basis for suggestion (3) above. In any case, the fundamental role played by the ocular dominance column boundaries in providing a local coordinate system for the cortical afferent geometry is the main point to be emphasized in the present model.

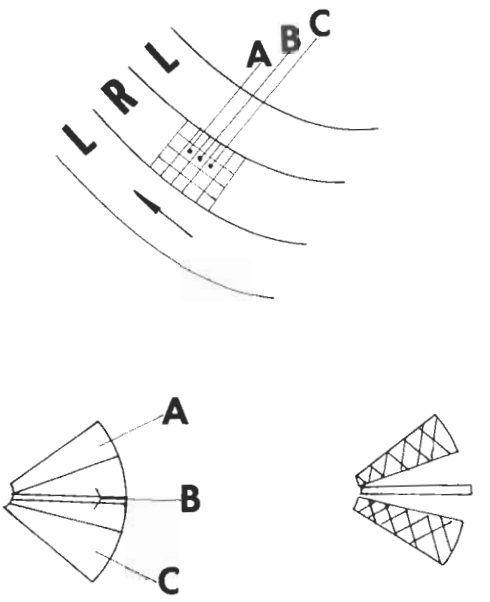

Fig. 4. A graphical simulation of the directional lateral inhibition operator of Equation (2). On the bottom, the image of Cells A and C are subtracted from Cell B, with the results shown on the right: an "excitatory center" is produced, with "inhibitory flanks". This simple differencing, superimposed on a complex logarithmic mapping, would cause both the inhibitory and excitatory fields of the cell to rotate together, i.e. sequence regularity. The direction of intra-cortical inhibition need not change, since the underlying mapping is effectively "rotating". The letters L, R, L refer to the ocular dominance columns which are schematically shown at the top

Sequence Regularity and Orientation Columns

The complex logarithmic structure for the hypercolumn of Figure 2 provides a sequence regularity property, as shown in Figure 5. All cells in a slab perpendicular to the direction of lateral inhibition (i.e. along ocular dominance column boundaries) will have receptive fields that are "tilted" by the same amount. Equal linear steps along the direction of lateral inhibition i.e. parallel to the ocular dominance column boundaries, will result in equal angular changes in orientation tuning. The orientation columns are specified indirectly, by a combination of directional cortical inhibition and afferent geometry. They need not have a direct anatomical substrate, and, in fact, none has been found to date. The principal point that emerges from this analysis is that the ocular dominance column boundaries are of central importance in organizing the cortical geometry.

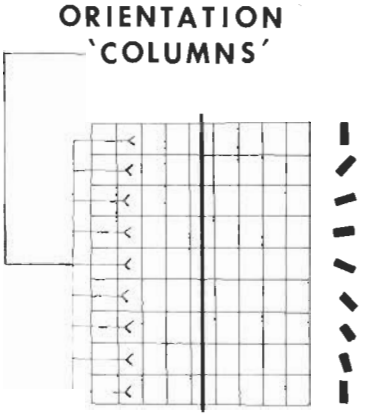

Fig. 5. Orientation "columns" would exist, by virtue of the afferent logarithmic geometry and the lateral inhibition operator suggested in this paper. These "columns" would not have an observable anatomical substrate, but would instead be the indirect result of the cortical afferent geometry

Ocular Dominance Distributions and the Bufon Needle Problem

The distribution of cells in the primate visual cortex with respect to binocular excitatory input forms a continuum with the percentage of binocular cells, relative to monocular cells, reported as 60% (Hubel and Wiesel, 1968), 43% (Poggio, 1972), and 49% (Schiller et al., 1976a), for the classification of "S" type cortical cells. Under the assumption that binocular excitatory input arises in the primate via summation across ocular dominance column boundaries, it is possible to relate the ocular dominance distribution (binocularity) to the average cell size and shape, and the width of the ocular dominance columns. The "Bufon Needle" problem refers to the calculation of the probability ("p") that a "needle" of length $2l$, when dropped on a parallel grid of ruled lines of spacing $2a$, will intersect a line of the grid. The "Bufon Needle" has been generalized to the case of a convex polygon of perimeter $2S$ intersecting a grid of parallel lines, and the corresponding probability is: (Gnedenko, 1967).

$$\varrho = \frac{s}{\pi a}. \tag{3}$$

Identifying the "polygon" as the dendritic tree of a cortical cell, the parallel grid as the ocular dominance column strips (Fig. 1) and the probability of intersection of the polygon with the grid as the percentage of binocular cells, then it is possible to get a simple estimate of the ratio of binocular to monocular cells. Substituting the value of 500 μ for the width of the grid (Levay et al., 1975) and a dendritic tree of average rectangular cross section 250 μ × 160 μ (Colonnier, 1963) then (3) yields a probability of 52%, which is in fair agreement with the experimental measurements of Hubel and Wiesel (1968), Poggio (1972), and Schiller et al. (1976a). Schiller's estimate of 49% binocularity refers to his category of "S" type cortical cells; his category of "CX" type cells showed 89% binocularity. Under the assumption that (3) is a valid estimate of binocularity, this would imply a dendritic tree, for Schiller's "CX" type cells, of 420 μ × 280 μ. In the "Bufon Needle" problem, the shape of the polygon is irrelevant; only the perimeter enters the equation, so that these rough estimates are not sensitive to the characterization of the cell dendritic tree as "cruciform" (Colonnier, 1963). Thus, the size of the cortical dendritic tree's and the spacing of the ocular dominance columns provide a clear prediction for the relationship of cortical histology to cortical binocular neurophysiology, and this prediction is accessible to direct experimental test.

Binocular Disparity Tuning

Cortical cells in the visual cortex of the cat tend to have a horizontal component of disparity in the location of their left and right eye receptive fields. Because of this trigger feature of disparity, it has been speculated that these cells function as "feature detectors" for stereoscoptic depth perception (Barlow et al., 1967). In the primate, Hubel and Wiesel (1970) have found two types of binocular depth cells, which they termed "ordinary" and "depth" type cells. Ordinary cells show a moderate summation of stimulation to the two eyes. They fire in response to monocular and binocular stimulation, and have their receptive fields in corresponding parts of the two retinal projections: they have zero measurable disparity. All cells in area 17 are "ordinary" type cells. The second category of "depth" cells give a weak response to stimulation of either eye alone, but have both a horizontal and vertical component to their disparity. In area 18, approximately equal numbers of "ordinary" and "depth" type cells occur, beyond 3–4° from the foveal representation. The salient feature of the binocular organization of area 18 is the linking of receptive field structure to binocular disparity. The disparity of "depth" cells is in a direction perpendicular to the direction of orientation tuning. Thus, vertically oriented cells have a horizontal disparity, horizontal cells have little measurable disparity, and obliquely oriented cells have both a vertical and horizontal component of disparity. Neighboring "depth" cells tend to have the same disparity, and "ordinary" and "depth" cells are arranged in clusters, or columns, on a scale which is larger than that of the "orientation columns".

The qualitative and quantitative description of the binocular trigger features of area 17 and area 18 is highly detailed, and provides a good test of the local

structure proposed in Figure 2 of this paper. If cortical trigger features arise in general from dendritic summation of this afferent geometry, then these very well described binocular trigger features should emerge naturally from the present model. A strong hint that this is the case derives from noting that there are basically two types of ocular dominance column boundaries. Type 1 boundaries lie between a left and right ocular dominance column *within* a single hypercolumn (i.e. referring to corresponding parts of the left and right retina). Type 2 boundaries lie between a left and right hypercolumn belonging to *adjacent* hypercolumns (i.e. referring to retinal positions that are shifted with respect to one another). Summation across Type 1 boundaries results in "ordinary" type cells, i.e. with no disparity, while summation across Type 2 boundaries results in "depth" type cells, since the shifted receptive fields of adjacent hypercolumns would be expected to contribute some disparity to the left and right receptive fields. Furthermore, the 50/50% distribution of the two types of cells would then follow naturally from the equal numbers of the two types of ocular dominance column boundaries, and the clustering together of the two types of cells would be explained also.

In order to illustrate this suggestion, a specific model must be assumed for the "packing" of neighboring hypercolumns. The basic hypercolumn structure is indicated in Figure 2. The cylindrical topological structure of Figure 2 (top) yields results that are substantially the same, and simpler to work out, than the non-oriented logarithmic structure of Figure 2 (bottom). If this "Moebius Strip" mapping is used, then the "packing" of neighboring hypercolumns must be as in Figure 6, in order for "Type 1" cells to have identical receptive fields in the left and right eye visual fields.

The cortex may be "tessalated" by using the mapping of Figure 2 (bottom) for the left eye set of ocular dominance columns, and "flipping" the mapping of Figure 2 (bottom) for the right eye set of ocular dominance columns, as shown in Figure 6. The Points A–D of Figure 2 are reproduced in this figure. The right eye ocular dominance column is lightly shaded, and two adjacent hypercolumns are shown in the figure. Cells X–Z (indicated by heavily shaded rectangles) straddle Type 1 ocular dominance column boundaries. The left and right eye receptive fields are shown in Figure 6, and these "ordinary" cells will have identical receptive fields. Cells U–W straddle Type 2 ocular dominance boundaries, and these "depth" type cells will have receptive fields with components of disparity that depend entirely on the "shift" between the receptive fields of adjacent hypercolumns. This shift, shown by the vector S, in Figure 6, will have the receptive field structure indicated in the figure. *For a shift with a purely horizontal component*, the vertically oriented cells will have a

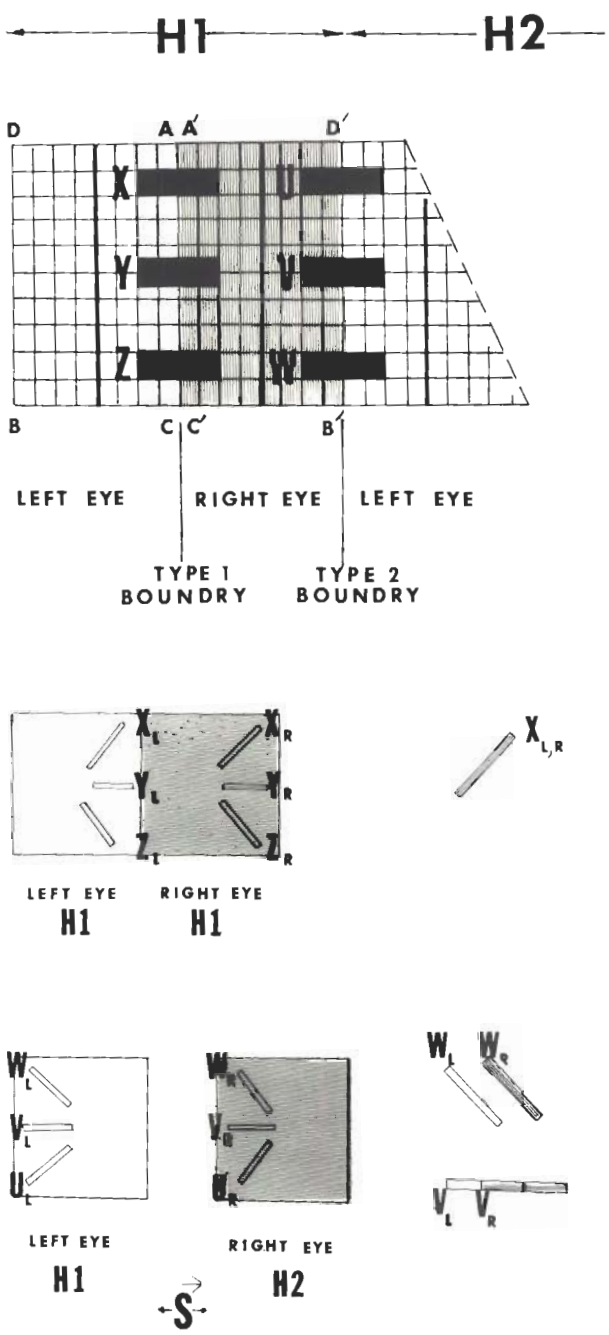

Fig. 6. On top, the placing of two adjacent ocular dominance columns, to form a single "hypercolumn" is shown. The Points A–D, have been retained from Figure 2 (bottom) and the non-oriented version of the logarithmic map is used for illustration. The left and right eye ocular dominance columns must alternately be mirror images, in order to achieve the correct mixture of binocular trigger features. The two types of ocular dominance column boundaries that exist are shown, and labelled "Type 1" (intra-hypercolumn) and "Type 2" (interhypercolumn). Thus, Cells X–Z would have "ordinary" properties and Cells U–W would have "depth" type properties. On the bottom is shown a representation of the receptive field images of these cells; the right eye is shaded, both in the cortical representation (top) and the visual field representation (bottom). H1 and H2 refer to neighboring hypercolumns, whose visual field representations are shifted by an amount S

purely horizontal component of disparity, and horizontally oriented cells will have little measurable disparity, in agreement with experiment (Hubel and Wiesel, 1970).

The direction of shift, S, of neighboring receptive fields is perpendicular to the border's of the ocular dominance columns. The vector S of Figure 6, which was chosen to agree with Hubel and Wiesel's observations (1970) would imply a direction of ocular dominance column boundaries that is vertical in the visual field. As was mentioned earlier (Fig. 1), the direction of ocular dominance column boundaries for the central 10° of visual field is *horizontal*. However, beyond 10°, the direction of the ocular dominance column's turns abruptly to the perpendicular direction (i.e. vertically in the visual field) (Levay et al., 1975). Within 3–4° of the foveal representation, there are few "depth" type cells, with the percentage increasing with further movement into the periphery. Apparently, most of the "depth" type cells were encountered further out in the periphery, and this may justify the presumed "vertical" orientation of the ocular dominance column boundaries shown in Figure 6.

There is a direct relationship between the cortical magnification factor (M, mm/degree), the magnitude and direction of the vector shift $\boldsymbol{S}$ describing the visual field projection of neighboring hypercolumns, the width of the ocular dominance columns (0.5 mm), and the vector disparity ($\boldsymbol{d}$, degrees):

$$\boldsymbol{d} = \frac{0.5\text{ mm}}{M\text{ mm/degree}} \cdot \boldsymbol{S} \tag{4}$$

where $\boldsymbol{S}$ is measured in a fraction of a receptive field (i.e. 50% overlap of neighboring r.f.'s). Equation (4) suggests a possible reason for the lack of "depth" type cells in area 17 of the monkey. The large magnification factor of the primate would make "depth" cells, arising from the geometric summation suggested in this paper, very difficult to detect experimentally. A value for cortical magnification of 6 mm/degree (Daniel and Whitteridge, 1962) for the central visual field would result, via Equation (4), in a predicted disparity of 1/24°, assuming a shift of 50% between neighboring hypercolumns. The striate magnification factor is still roughly 1 mm/degree at 10° of eccentricity ($d = 0.25°$). Although Hubel and Wiesel (1970) do not report on the range of eccentricity for which they searched in area 17 for "depth" type cells, (4) suggests that these cells would appear to be absent, except at fairly large eccentricity.

In the cat, the cortical magnification factor is roughly 5 times smaller than the primate, and so binocular disparity tuning should be easily detectable in area 17, which is the case. The cortical magnification factor in area 18 of the primate is considerably less than in area 17, due to the smaller tissue area; even in area 18, Hubel and Wiesel (1970) found "depth" type cells to be numerous in the more peripheral visual field. Thus, the lack of "depth" type cells in area 17 could be due to the experimental difficulty induced by the large value of the cortical magnification factor, in the primate.

Vorticity, the Navier-Stokes Equation and the Analytic Structure of the Cortical Map

In the previous discussion, a particular topology and tessalation of the cortical mosaic was *assumed*, which, together with the suggestion of local logarithmic structure, provides the proper mixture of monocular and binocular cortical trigger features. Specifically, a non-orientable ("Moebius strip") topology was proposed, to achieve symmetry about the local receptive field center, and adjacent left-eye—right eye hypercolumn patches were "flipped" with respect to one another, in order to achieve a 50-50% mixture of "ordinary" and "disparity" type binocular cells. However, it is possible to use the orientable cylindrical topology of Figure 2 (i.e. that of the global cortical map, which is the standard Riemann surface for the logarithm function), and to motivate the "flipping" of left and right eye local patches in a natural way that has the advantage of providing a single analytic function to describe both the local and global cortical structure. Moreover, this analytic (or technically, meromorphic) function has been presented in the literature of fluid mechanics as a description of the "Karman vortex street" (Rosenhead, 1929), and an analysis of the basis of vorticity in fluid mechanics provides potential insight into the nature of the developmental process, which is a direct extension of previous work relating neural development to the theory of potential flow (Schwartz, 1977b).

A meromorphic function (i.e. an analytic function) with a finite number of zeroes and poles (Ahlfors, 1966) which is both locally and globally complex logarithmic is:

$$\ln[cn\{\ln z, k\}] \tag{5}$$

where $cn(u, k)$ is a Jacobian elliptic function, and k is chosen so that the ratio of the real and imaginary semi-periods of the elliptic function are equal to the ratio of the spacing of zero's to zero's, and zero's to poles in the grid of logarithmic maps. This function is presented, and discussed, in Morse and Feshbach (1953, pp. 1242); it represents the complex electrostatic potential of an array of line charges placed between two conducting cylinders. Due to limitations of space, it is not possible to discuss in detail (5); it is merely stated, with reference to Morse and Feshbach (1953), that this particular meromorphic function describes a map which is both locally and globally logarithmic in its structure, and so

may be taken, following the arguments presented in this and previous (Schwartz, 1976, 1977a–c) papers, as a concise representation of the analytic structure of the retinotopic mapping of the primate striate cortex. The "flipping" of adjascent local cortical maps, which was *assumed* in the previous discussion, is a natural consequence of the analytic structure of Equation (5), since the local logarithmic structure of this mapping is represented alternately by $+\ln(z-z_0)$ and $-\ln(z-z_0)$, where z_0 is the local hypercolumn center. The alternating sign of the local logarithmic map therefore yields patches which are related by reflection through the local origin. Finally, a potentially important insight into the development of the striate cortex is provided by noting that (5) is related to the structure of an array of Karman vortex streets in fluid mechanics (Rosenhead, 1929), and suggests the possibility that the existence of rotating receptive field structure in the cortex is intimately related to the boundary conditions that are imposed by the regularly alternating ocular dominance strips of layer IV of the striate cortex. This statement will be briefly explained in the following section; the interested reader is referred to work currently in preparation for a more detailed account (Schwartz, 1977d).

A Karman vortex street is created by the passage of a bluff object through a viscid fluid, i.e. by the tip of a coffee spoon moving in water, or the tip of an airplane wing moving through air. The structure of a Karman vortex street is that of a series of logarithmic vortex patterns, spinning clockwise and anit-clockwise, in alternation (Fig. 7). The existence of vortex patterns in fluid flow may be traced to the existence of tangential discontinuities in the fluid velocity, and we note that velocity (i.e. the derivative of the complex potential) is equal to magnification factor, in the context of the primate retinotopic mapping (Schwartz, 1977a).

Again, in the context of the neural mapping, discontinuities in the magnification factor are clearly and obviously supplied by the alternating ocular dominance column structure of the cortical map. This situation is expressed by Rosenhead (1930): "... the effect ... of a surface of discontinuity (in a fluid flow) is to produce concentrations of vorticity at equal intervals along the surface...". These equally spaced vortex patterns are clearly similar to the pattern of cortical afferent input that has been suggested in the present paper, and the developmental significance of this remark may be interpreted in the light of previous discussions of the specification of visual connections in the vertebrate nervous system (Schwartz, 1977b). In this work, it was pointed out that the boundary conditions of the tissue surfaces of the primate retina and cortex (and the goldfish retina and optic tectum) are sufficient to encode the detailed structure of the receptotopic

Fig. 7. A photograph of a cylinder moving in a viscous fluid (Reynolds number = 250), with a Karman vortex street following in the wake. Reprinted from Theoretical Hydrodynamics, L. M. Milne-Thomson, MacMillan (1955)

mappings. provided that the mapping is a solution of the Laplace equation, i.e. that it is a "potential flow".

The mathematics of this statement is identical to that of the solution of the classical, inviscid, irrotational flow of a fluid (Morse and Feshbach, 1953). However, this characterization of the goldfish and primate retinotopic mappings describes the structure of the global mappings, and not the local mapping discussed at length in the present work. In order to introduce local logarithmic structure, it is necessary to extend the analogy of fluid flow from the simple description provided by the Laplace equation, to the more sophisticated representation of fluid flow provided by the Navier-Stokes equation, which includes the effects of vorticity, or rotational motion. The mathematical details of this program are non-trivial, since analytic solutions of the Navier-Stokes equation are few and far between. Nevertheless, insight into the nature of the solutions of this non-linear, partial differential equation may be obtained from the following approximation to the classical Navier-Stokes equation, which is valid for plastic flow, in which the effects of tangential

discontinuity are the dominant factor (i.e. low Reynolds number) (Campbell, 1973):

$$\nabla^2 \xi = 0$$

$$\xi = \nabla \times \boldsymbol{v} .$$

In this approximation, the Navier-Stokes equation indicates that the distribution of vorticity (ξ) is a solution to the Laplace equation, and hence the vorticity (which may be thought of as the density of local logarithmic structure) is distributed with a logarithmic pattern. This statement follows from the fact that the logarithm function is the solution to the Laplace equation with circular boundary conditions (Ahlfors, 1966).

Thus, the logarithmic pattern of logarithmic maps that is represented by (5), and which is suggested to represent the afferent input to the primate retinotopic mapping in the present work, may be thought of as a solution to the approximation to the Navier-Stokes equation of (5). Finally, it may be pointed out that the Karman vortex street is stable to small perturbations only for a pattern of vortex spacing (i.e. vertical/horizontal spacing) which is equal to 0.28 (Lamb, 1945). Thus, there is a natural scale associated with the formation of a Karman vortex street, and this scale is not inconsistent with the scale of the primate cortex, using the values of ocular dominance column width (300–500 μ) and hypercolumn length (approximately 1000 μ) suggested by Hubel and Wiesel (1974). Quantitative measurement of the scale of the cortical pattern could thus supply circumstantial evidence in support of the Karman vortex street model of the cortical map.

The details of cortical trigger features, following from the Karman vortex model of the cortical map, yield a ratio of "ordinary" to "disparity" type cells of 25/75%, as may be verified by the reader, following Figure 6. This value is not in agreement with the 50/50% ratio reported by Hubel and Wiesel (1974). For this reason, the alternate tessalation of the cortex presented earlier in this paper, may be considered, particularly since the binocular trigger features of the primate cortex have not been extensively studied. The potential importance, with respect to neural development, of the discussion based on the Navier-Stokes equation, and the Karman vortex street, justify its consideration as a candidate for the description of the afferent structure of the cortex. Through this approach the two striking features of cortical phenomenology (i.e. ocular dominance columns and sequence regularity) are unified into a single mathematical description which is relevant to the anatomy, physiology, and development of the cortex.

Cortical Trigger Features and the Feature Detector Hypothesis

Clearly, the orientation of a geometric approach to the description of the anatomy and neurophysiology of the striate cortex is to underplay the functional importance of trigger features. In particular, what is to be made of the common identification of cortical trigger features with the psychological process of feature extraction? Feature extraction refers to the representation of a complex sensory stimulus by a set of features which retain the salient information, but which discard redundant aspects of the stimulus (Werner, 1974). One of the principal goals of sensory neurophysiology has been to identify neuronal mechanisms that may be related to the psychological process of feature extraction. The view that the existence of well defined neuronal trigger features may subserve the psychological process of feature extraction has been both defended (Barlow, 1972) and rejected (John and Schwartz, 1978). This doctrine has been carried to extreme lengths: Barlow (1972) has suggested that complex percepts may be encoded by the firing of one or a few high level "cardinal cells". The thrust of this extreme single cell feature detector position is to reduce complex psychological processes (i.e. feature extraction) to a level which is accessible, at least in principle, to neurophysiological measurement. Since trigger features are readily measured, a theoretical position that is committed to the properties of single neurons is well suited to current experimental strategies. However, there are severe logical problems with this position. Very few neurophysiologists would consent to do a double blind study in which the firing rate of a single neuron in the cortex was used to guess at the nature of an unknown stimulus. The firing rate of cortical neurons depends in general on a wide variety of factors, such as contrast, stimulus orientation, stimulus length, stimulus velocity, binocular disparity, vestibular stimulation, and auditory stimulation. It is clear that the unambiguous identification of a stimulus must in general be a collective property of the firing of many neurons in many anatomical brain regions (John and Schwartz, 1978).

Visual Information Processing

Remapping the visual scene via the complex logarithmic mapping has a number of powerful advantages with respect to pre-processing peripheral visual information. Casasent and Psaltis (1976), in an optical computer application, have shown that complex logarithmic pre-processing possesses useful size-invariance and rotation invariance properties, discussed in detail

by Chaikin and Weiman (1977), and which are derived and illustrated in the context of the global logarithmic structure of the primate cortex, by Schwartz (1977a). In effect, the complex logarithm function provides a sort of natural "size zooming" capability, a fact which could have importance with respect to a number of perceptually relevant phenomena.

The fact that the left and right retinal images are remapped to the visual cortex (the earliest site of binocular interaction in the primate) by the complex logarithmic mapping is of crucial importance to any possible cross-correlational basis of stereopsis. As the vergence and version angles of the eyes change, the instantaneously fixated image will have different size and rotational projections in the two eyes. It is well known that cross-correlation is very sensitive to size and rotation differences in the templates that are to be matched (Duda and Hart, 1973). Casasent and Psaltis have shown that size dilatations of 1% and rotations of 1° cause a 20 decibel drop in signal-to-noise ratio, in an optical computer cross-correlation application. *The solution proposed by Casasent and Psaltis (1976) is a complex logarithmic remapping of the template.* Following this pre-processing step, which they perform electronically on a digitized image, there is no signal-to-noise loss following size dilatations of up to 100%. Thus, if cross-correlation is to play a role in the neural basis of stereopsis, it is necessary to perform an initial size and rotation normalization on the retinal input. This is provided automatically by the anatomical structure of the retinotopic mapping (Schwartz, 1976, 1977a, b).

Finally, the suggestion that the direction of intracortical lateral inhibition lies predominantly parallel to the ocular dominance column boundaries (i.e. the horizontal direction in the visual field for the central 10°) would seem to have significance for stereopsis as well: the left and right eye "cortical images" differ by a predominantly horizontal disparity (referred to the visual field) and the cortical lateral inhibition operator proposed in this paper would act to "sharpen" this image disparity, just as the circularly symmetric lateral inhibition operator of the retina serves to "sharpen" the contours of the monocular projection of the visual field.

Acknowledgement. I am grateful to C. Roy John for support and encouragement in the preparation of this work.

References

Ahlfors, L.: Complex analysis. New York: McGraw Hill 1966

Albus, K.: A quantitative study of the projection area of the central and paracentral visual field in area 17 of the cat. Exp. Brain Res. **24**, 159—179 (1975)

Barlow, H.B.: Single units and sensation: a neuron doctrine for perceptual psychology. Perception **1**, 371–380 (1972)

Barlow, H.B., Blakemore, C., Pettigrew, J.D.: The neural mechanisms of binocular depth discrimination. J. Physiol. **193**, 327–342 (1967)

Campbell, R.G.: Foundations of fluid flow theory. Massachusetts: Addison Wellsely 1973

Casasent, D., Psaltis, D.: Position, rotation, and scale invariant optical correlation. Appl. Opt. **15**, 1795–1799 (1976)

Chaikin, G., Wieman, C.: Submitted to Computer Graphics and Information Processing (1977)

Colonnier, M.: The tangential organization of the visual cortex. J. Anatomy **98**, 327—344 (1964)

Creutzfeld, O.D., Kuhnt, U., Benevento, L.A.: An intracellular analysis of cortical neurons to moving stimuli: responses in a cooperative neuronal network. Exp. Brain Res. **21**, 251—274 (1974)

Daniel, P.M., Whitteridge, D.: The representation of the visual field on the cerebral cortex in monkeys. J. Physiol. **159**, 203–221 (1961)

Duda, R.O., Hart, P.E.: Pattern classification and scene analysis. New York: Wiley 1973

Fischer, B.: Overlap of receptive field centers and representation of the visual field in the optic tract. Vision Res. **13**, 2113—2120 (1973)

Gnedneko, B.V.: Theory of probability. New York: Chelsea 1967

Hubel, D.H., Wiesel, T.N.: Receptive fields, binocular interaction and functional architecture in the cats visual cortex. J. Physiol. (Lond.) **160**, 106—154 (1962)

Hubel, D.H., Wiesel, T.N.: Cortical and callosal connections concerned with the cortical meridian of visual fields in the cat. J. Neurophysiol. **30**, 1561–1573 (1967)

Hubel, D.H., Wiesel, T.N.: Receptive fields and functional architecture of monkey striate cortex. J. Physiol. (Lond.) **195**, 215–243 (1968)

Hubel, D.H., Wiesel, T.N.: Steroscopic vision in macaque. Nature **225**, 41—44 (1970)

Hubel, D.H., Wiesel, T.N.: Laminar and columnar distribution of geniculo-cortical fibers in the macaque monkey. J. comp. Neurol. **146**, 421—450 (1972)

Hubel, D.H., Wiesel, T.N.: Sequence regularity and geometry of orientation columns in the monkey striate cortex. J. comp. Neurol. **158**, 267—293 (1974)

John, E.R., Schwartz, E.L.: Neurophysiology of sensory information processing and cognition. Ann. Rev. Psychol. **29**, (1978) (in press)

Julesz, B.: Foundations of cyclopean perception. Chicago: University of Chicago Press, 1971

Lamb, Sir Horace: Hydrodynamics. New York: Dover 1945

Levay, S., Hubel, D.H., Wiesel, T.N.: The pattern of ocular dominance columns in macaque visual cortex revealed by a reducea silver stain. J. Comp. Neurol. **159**, 559–576 (1975)

Marin-Padilla, M.: Pre-natal and early post-natal ontogenesis of the human motor cortex: a golgi study. Brain Res. **23**, 185 (1970)

McIlwain, J.T.: Large receptive fields and spatial transformations in the visual system. Int. Rev. Physiol. **10**, 223—248 (1976)

Panofsky, W., Phillips, M.: Classical Electricity and Magnetism. Reading Mass: Addison and Wellesly, 1962

Rosenhead, L.: The Karman street of vortices in a channel of finite breadth. Phil. Trans. Roy. Soc. A**228**, 275—329 (1929)

Rosenhead, L.: The formation of vortices from a surface of discontinuity. Proc. Roy. Soc. A**134**, 170—192 (1931)

Rose, D.: The hypercomplex cell classification in the cats striate cortex. J. Physiol. **242**, 123—125 (1974)

Sanderson, K.J.: Visual field projection columns and magnification factors in the lateral geniculate body of the cat. Exp. Brain Res. **13**, 159—177 (1971)

Schwartz, E.L.: The analytic structure of the retinotopic mapping of the striate cortex. Neuroscience Society Abstracts, Sixth Annual Meeting, p. 1133 (1976)

Schwartz, E.L.: Spatial mapping in the primate sensory projection: analytic structure and relevance to perception. Biol. Cybernetics **25**, 181–194 (1977a)

Schwartz, E. L.: The development of specific visual connections in the monkey and the goldfish: outline of a geometric theory of receptotopic structure. J. Theor. Biol. (1977b in press)
Schwartz, E. L.: Afferent geometry in the primate visual cortex. Soc. for Neuroscience Abstracts (1977c)
Schwartz, E. L.: Turbulent mixing of binocular input in the striate cortex (In preparation, 1977d)
Schiller, P. H., Finlay, B., Volman, S. F.: Quantitative studies of single cell properties in monkey striate cortex II: orientation specificity and ocular dominance. J. Neurophysiol. **39**, 1320—1333 (1976a)
Schiller, P. H., Finlay, B., Volman, S. F.: Quantitative studies of single cell properties in monkey striate cortex V: Multivariate statistical analyses and models. J. Neurophysiol. **39**, 1362—1374 (1976b)
Spivak, J.: Differential Geometry Vol. I. Berkeley: Publish or Perish Press 1970
Springer, G.: Introduction to Riemann surfaces. Reading: Addison Wellesly 1957
Werner, G.: The topology of the body representation in the somatic afferent pathway. In: The Neurosciences Second Study Program, Schmidt, F. O., ed, New York: Rockefeller University Press 1970
Werner, G.: Neuronal information processing with stimulus feature extractors. In: The Neurosciences Third Study Program, ed. Schmidt, F. O., Worden, F. G., New York: Rockefeller University Press 1974

Received: May 24, 1977

Dr. E. L. Schwartz
Brain Research Lab.
Dept. Psychiatry
N.Y.U. Medical Center
550 1st Ave
New York, NY 10016, USA

Note added in proof. It was suggested in this paper that quantitative measurement of the sequence length and ocular dominance column spacing could supply additional support for the Karman vortex street model of the cortical map. After this paper had gone to press, Wiesel, Hubel and Stryker [Society for Neuroscience Abstract No. 1863 (1977)] reported accurate measurements for both these numbers: the primate ocular dominance column spacing is 385 microns, and the sequence length for 360 degrees (i.e. two vertical stripes, using the orientable topology for the local cortical map of this paper) is 1140 microns. The ratio of these measurements is 0.34, compared with the von Karman ratio of 0.28 predicted in this paper. Also, Stryker, Hubel and Wiesel [Society for Neuroscience Abstract No. 1852 (1977)] report a measurement in the cat for 360 degrees of sequence length (i.e. two vertical stripes) of 1740 microns, but do not report a measurement of the ocular dominance column width. Using a value of 500 microns for the ocular dominance column width in the cat [Hubel and Wiesel, J. Physiol. **165**, 559 (1963)] would yield a "von Karman ratio" for the cat of 0.29. Also, the classical von Karman ratio is calculated for idealized point vortices; when vortex structure of finite size is examined, the stability range may vary within a region centered at 0.28 [Zabusky, N. Coherent Structure in Fluid Dynamics, presented at Orbis Scientiae (1977)]. Thus, both the primate and cat cortex exhibit scaling that is consistent with the von Karman stability criterion (Lamb, 1945). Finally, the elliptic function presented in this paper, which has been used to represent a Karman vortex street velocity potential in the literature (Rosenhead, 1931) is multiple valued; each cortical hypercolumn may be thought of as a single sheet of the Riemann surface of this function. By this means, it is possible to have a convenient functional model for the geometric structuring of the cortical map that is suggested in this paper.